DOI:10.26524/KRJ303

Kong. Res. J. 6(2): 61-65, 2019
Publisher: Kongunadu Arts and Science College, Coimbatore.

http://krjscience.com

RESEARCH ARTICLE

MIXED METAL OXIDE MESOPOROUS NANOPARTICLES FOR ENVIRONMENTAL REMEDIATION

Nithya Davis[1], P. Usha Rajalakshmi[1] and T. Sakthivel[2,*]

[1]Department of Physics, Avinasilingam Institute For Home Science and Higher Education For Women1, Coimabatore – 641 043, Tamilnadu, India.

[2]Department of Zoology, Kongunadu Arts and Science College, Coimbatore- 641 029, Tamil Nadu, India.

ABSTRACT

Mesoporous mixed metal oxides ($SnO_{2(x)}$ -$TiO_{2\ (1-x)}$, x= 0.75,0.50 and 0.25) were synthesized by evaporation induced self assembly using cationic surfactant, Cetyl Trimethyl Ammonium Bromide (CTAB) as the structure directing agent. The small angle X-ray diffraction pattern of mesoporous SnO_2 and SnO_2-TiO_2 mixed metal oxides revealed the presence of well defined mesostructure in the metal oxides. The mixed metal oxide system has crystallized in orthorhombic structure, resembling the host lattice. Mesopore channels were collapsed upon calcinations at 550°C. The optical absorption of the SnO_2 has been extended into the visible region upon incorporation of "Ti". A remarkable enhancement of the photocatalytic degradation efficiency (60%) of ($SnO_{2(0.5)}$ -$TiO_{2\ (0.5)}$ was observed against aqueous solution of methylene blue dye.

Keywords: SnO2, TiO2, Metal oxide, Semiconductor, Photocatalysis, Environmetal remediation.

1. INTRODUCTION

Metal oxides are prospective materials for applications in various fields such as solar energy conversion, photocatalysis, electrochemical catalysis, lithium/sodium ion batteries, field effect transistors and super capacitors [1-17] and have been intensively studied due to their inherent chemical stability, abundance, low cost and environmental friendliness. Metal oxide nanostructures are being widely used in place of bulk counterparts as the unique morphology, surface structure and optoelectronic characteristics associated with the nanostructures are uniquely enhancing the performance devices. Rational design and reproducible synthesis of stable nanomaterials of particular shape, size and microstructure is highly desirable. In particular, synthesis of porous metal oxides with ordered pore structures, as required for photocatalytic applications is remaining a challenging task. Notably, tin oxide (SnO_2), a wide band gap semiconductor, has appropriate optoelectronic characteristics suitable for photocatalytic applications but SnO_2 nanostructures produced by solvothermal / hydrothermal methods have always exhibited a fairly low specific surface area(<50 $m^2\ g^{-1}$)[18]. Hence it is imperative to improve the synthesis strategies to produce mesoporous SnO_2 with improved specific surface area. Surfactant templating strategy for the synthesis of non-silica based mesostructures, mainly metal oxides in which both positively and negatively charged low molecular weight surfactants are widely being used for the synthesis of mesoporous metal oxide nanoparticles. It was found that charge density matching between the surfactant and the inorganic species is important for the formation of the organic-inorganic mesophases. In the recent past efforts have been made to employ the potential of mesoporous metal oxides/metal oxide nanocomposites for environmental remediation [19-24].

In the present work, an attempt has been made to synthesize Mesoporous Tin Oxide (SnO_2) by Evaporation Induced Self Assembly and to extend/optimise the synthesis procedure to synthesize SnO_2 –TiO_2 mixed metal oxide system. Attempts have been made to analyse the photocatalytic activity of the mesoporous metal oxides for the degradation of methylene blue.

2. MATERIALS AND METHODS

In the present work following methodology adopted for the synthesis of mesoporous SnO_2 and $SnO_{2(x)}$ -$TiO_{2\ (1-x)}$ mixed metal oxides by Evaporation-Induced Self-Assembly.

2.1. Synthesis of Ordered Mesoporous Titania

Mesoporous tin oxide (SnO_2) is synthesized using cationic surfactant, Cetyl Trimethyl Ammonium Bromide (CTAB) as the structure directing agent and tin tetrachloride (1.0 M in methylene chloride, Sigma Aldrich) and titanium tetrachloride (1.0 M in methylene chloride, Sigma Aldrich) as the source for tin and titanium respectively. The surfactant solution is obtained by dissolving 2.5 g of CTAB in 50 ml of cyclohexanol (Sigma Aldrich) and the solution (Sol A) is

*Correspondence: Sakthivel, T., Department of Zoology, Kongunadu Arts and Science College, Coimbatore – 641 029, Tamil Nadu, India. E.mail: sathivelunom@gmail.com

continuously stirred for 2 h during which 3.5 ml of concentrated HCl is added drop wise. To the resulting solution A, 10 ml of tin tetrachloride is added drop wise and stirred for 4 hours. The resulting solution thus obtained is made as a thin layer and kept in hot air oven maintained at 60°C for 4 days. The solid product obtained is calcined in a tubular furnace at a temperature of 550°C for 6 hours at a heating rate of 1°C / minute with air flow. The sample is coded as MSNO-43. Similarly mixed tin – titanium metal oxides ($SnO_{2(x)}$ -$TiO_{2\ (1-x)}$) are prepared by incorporating suitable amount of tin and titanium precursors. The resulting samples are coded as MSNO - 43 (SnO_2), MSTO - 43 ($SnO_{2(0.75)}TiO_{2(0.25)}$), MSOTO - 43 ($SnO_{2(0.5)}TiO_{2(0.5)}$),MSTO - 43 ($S_2nO_{2(0.25)}TiO_{2(0.75)}$), MTIO - 43 ($TiO_2$) .

2.2 Material characterization

The characteristics of materials prepared in present work were systematically analyzed using X-Ray Diffractometer (Rigaku Miniflex II), High Resolution Transmission Electron Microscope (HRTEM, JEOL JEM 2100, operated at an accelerating voltage of 120 kV), UV-Vis. Spectrophotometer (JASCO, V-650).

2.3 Photocatalytic activity

The synthesized SnO_2 and metal oxide were tested for photocatalytic degradation of methylene blue. Around 0.2g of the catalyst was suspended in quartz cell along with 200ppm, 5ml aqueous solution of the dye. Prior to light irradiation, the suspension was stirred for 30 minutes in dark to attain the absorption- desorption equilibrium. The sample was irradiated using natural sunlight. At periodic intervals, 5ml aliquots were taken from the system and analysed using UV-Vis spectrophotometer.

3. RESULTS AND DISCUSSION

The small angle X-ray diffraction pattern of mesoporous SnO_2 and SnO_2-TiO_2 mixed metal oxides are shown in figures 1-5. The presence of well defined diffraction peak centered at 2θ of 0.7° (Fig.1) is indicative of the formation of long range ordered pore structure and the peaks are arising from (100) reflections associated with 2D hexagonal (*P6mm*) arrays of uniform mesopores [25].

The X-ray diffraction pattern of mesoporous SnO_2 prepared in the present work is shown in figure 6. The samples were found to have crystallized in orthorhombic structure, the formation of which is favored at higher temperatures [26]. XRD pattern of TiO_2 reveals the formation of a mixed phase containing anatase, rutile and brookite.The XRD pattern of mixed metal oxides prominently featured characteristic features of orthorhombic SnO_2 (JCPDS Card No. 78-1063).

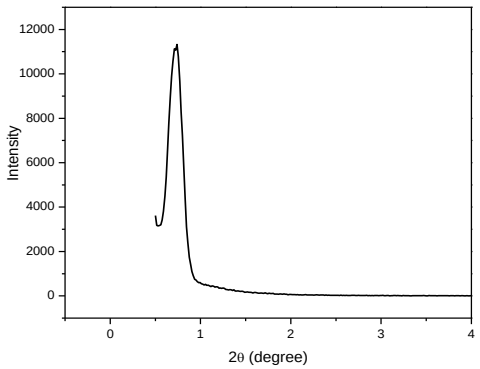

Fig. 1. Small angle XRD pattern of MSNO-43

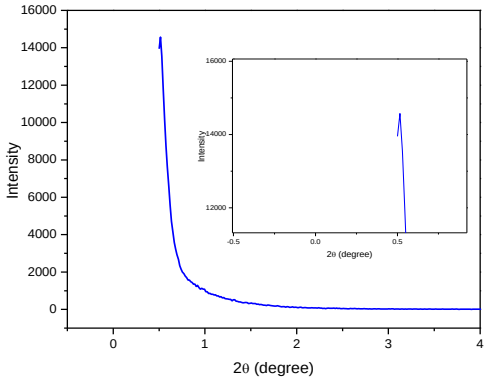

Fig. 2. Small angle XRD pattern of MSTO-43

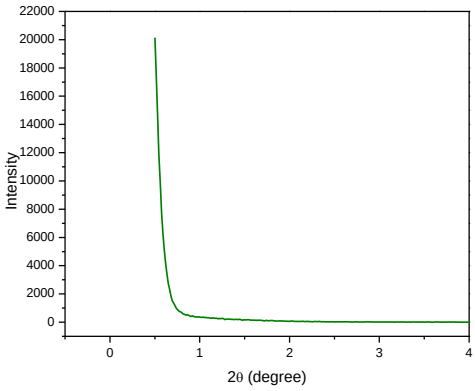

Fig. 3. Small angle XRD pattern of MSOTO-43

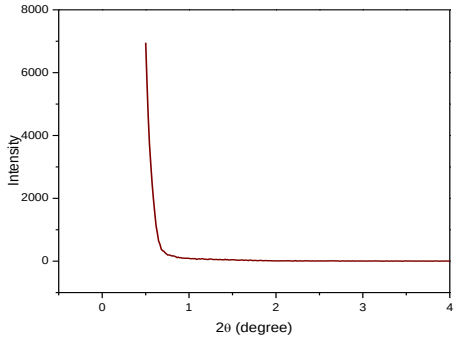

Fig. 4. Small angle XRD pattern of MTSO-43

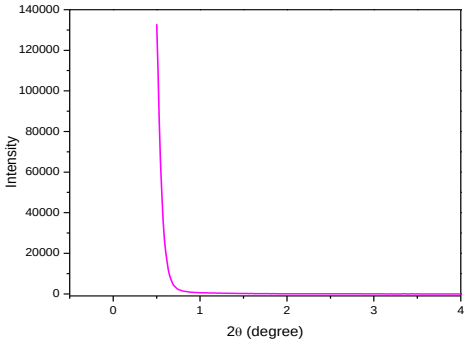

Fig. 5. Small angle XRD pattern of MTIO-43

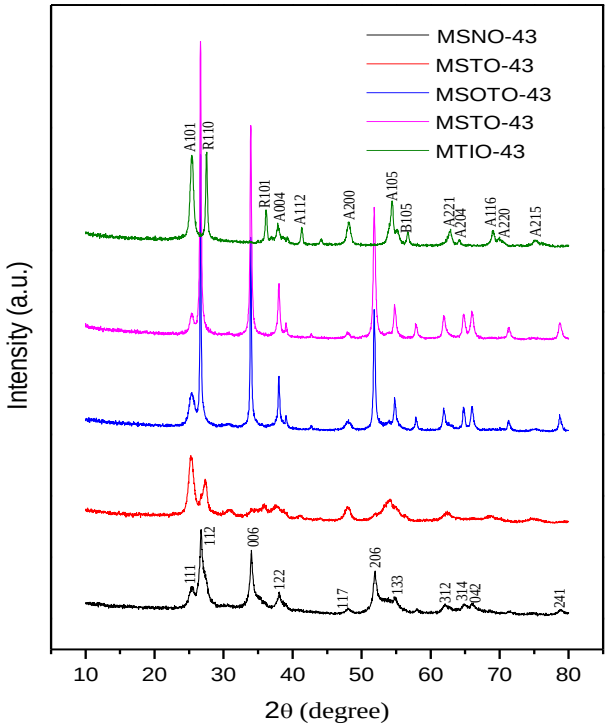

Fig. 6. XRD pattern of mesoporous SnO2 and SnO2-TiO2 mixed metal oxides

The presence of pore channels in the porous metal oxides are noticed from the High Resolution Transmission Electron Micrographs (Figure 7 a and b) of the samples, MSNO-43 and MSOTO-43. The pore structure has been observed to collapse upon calcinations at 550°C.

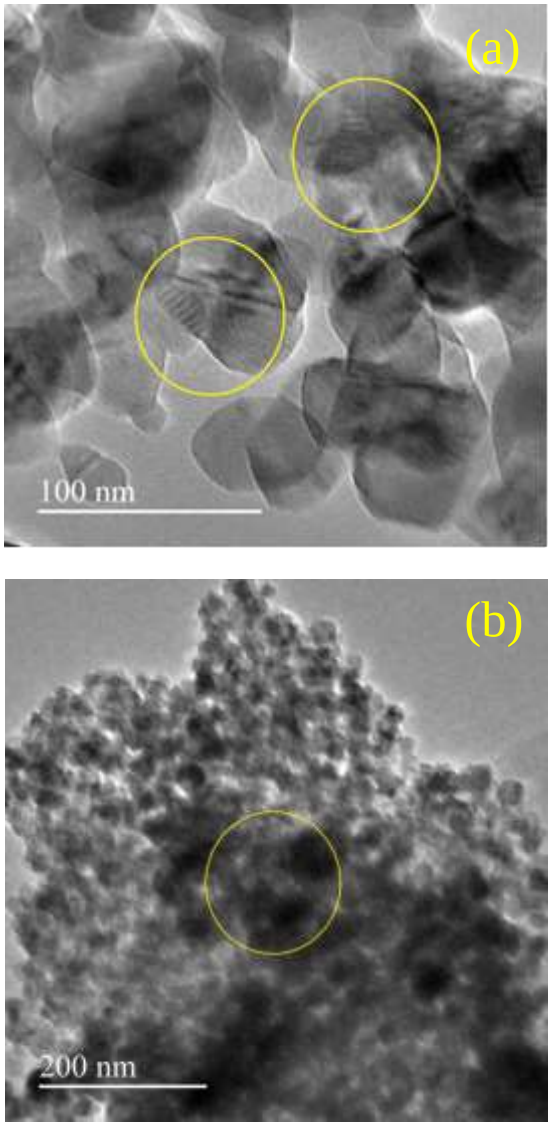

Figure 7. HRTEM images of mesoporous SnO_2 and SnO_2-TiO_2 mixed metal oxides

The diffuse reflectance UV-Vis. spectra of mesoporous SnO_2 and SnO_2-TiO_2 mixed metal oxides are shown in Fig. 8. The mixed metal oxides (MSOTO-43 and MSTO-43) exhibited enhanced visible light absorption which can be ascribed to the presence of defect levels within the band gap of the material.

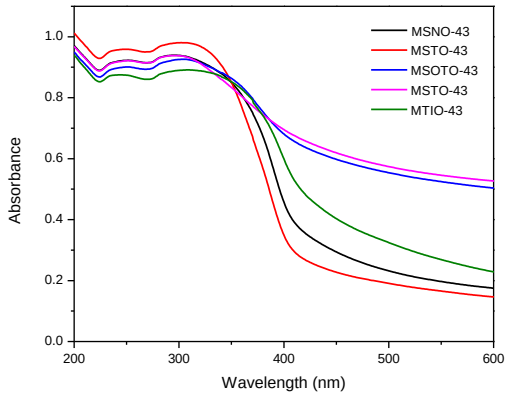

Fig.8. Diffuse reflectance UV-Vis. spectra of SnO_2 and SnO_2-TiO_2 mixed metal oxides

The photocatalytic efficiency of mixed metal oxide nanoparticles are analysed against the photocatalytic degradation of methylene blue. The optical absorption characteristics of the dye without the photocatalyst and with photocatalyst are recorded using UV – Vis spectrophotometer. The photocatalyst is added to the aqueous solution of the dye and the reaction was allowed to proceed under direct sunlight. The concentration of the dye and the absorbance of the reactant at 390 nm (where has it absorbance maxima) are evaluated from Beer – Lambert law after specified reaction time of 20, 40 and 60 minutes. The photocatalytic efficiency of the dye is calculated by noting the variation in the concentration of the dye after a specified reaction time (C) with respect to the concentration of the dye at time t = 0 (C_0).

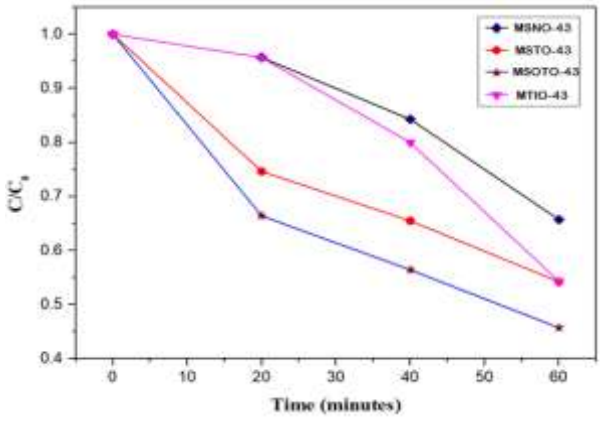

Figure 9. Photocatalytic Performance of SnO_2 and SnO_2-TiO_2 mixed metal oxides

Fig. 9 shows the variation of $C/C_0$with respect to time. SnO_2 particles photocatalytically degraded methylene blue (MB) under visible light radiation by 30%. Since the mesoporous structure enhances the surface area of the semiconductor widely, remarkable enhancement in the photocatalytic efficiency of the mesoporous photocatalyst was observed. Photocatalytic efficiency of mesoporous $SnO_{2(0.5)}$ -$TiO_{2\,(0.5)}$ (MSOTO-43) nanoparticles was the highest (60%) and further doping has been found to decrease the photocatalytic efficiency. The creation of defect level in the host metal oxide due to formation of mixed metal oxide system plays a pivotal role in enhancing the visible light absorption and in increasing the lifetime of photogenerated charge carriers.

4. CONCLUSION

Mesoporous tin oxide and $SnO_{2(x)}$ -$TiO_{2\,(1-x)}$ mixed metal oxides were synthesized by evaporation induced self assembly method. Systematic analysis on the characteristics of the material revealed the formation of crystalline and mesoporous nanoparticles. The $SnO_{2(x)}$ -$TiO_{2\,(1-x)}$ exhibited visible light activity which originates from the creation of electronic states in the band gap of the material. The enhanced optoelectronic characteristics of the system $SnO2_{(0.5)}$ -$TiO_{2\,(0.5)}$ extends the potential of material for environmental remediation through the treatment of organic pollutants such as 4-Chlorophenol and synthetic dyes.

REFERENCES

1. Kim, H.R., K.I. Choi, J.H. Lee and S.A. Akbar, (2009). Highly Sensitive and Ultra-fast Responding Gas Sensors Using Self-assembled Hierarchical SnO_2 Spheres. *Sens. Actuators B* **136**: 138-143.
2. Kuang, Q., C. Lao, Z.L. Wang, Z. Xie and L. Zheng, (2007). High-Sensitivity Humidity Sensor Based on a Single SnO_2 Nanowire. *J. Am. Chem. Soc.*, **129**: 6070-6071.
3. Liu, Y., Y. Jiao, Z. Zhang, F. Qu, A. Umar and X. Wu, (2014). Hierarchical SnO_2 Nanostructures Made of Intermingled Ultrathin Nanosheets for Environmental Remediation, Smart Gas Sensor, and Supercapacitor Applications. *ACS Appl. Mater. Interfaces* **6**: 2174-2184.
4. Lipeng, Q., X. Jiaqiang, D. Xiaowen, P. Qingyi, C. Zhixuan, X. Qun and L. Feng, (2008). The Template-free Synthesis of Square-shaped SnO_2 Nanowires: the Temperature Effect and Acetone Gas Sensors. *Nanotechnology* **19**: 185705.
5. Dong, Z., H. Ren, C.M. Hessel, J. Wang, R. Yu, Q. Jin, M. Yang, Z. Hu, Y. Chen, Z. Tang, H. Zhao and

D. Wang, (2014). Quintuple-Shelled SnO_2 Hollow Microspheres with Superior Light Scattering for High-Performance Dye-Sensitized Solar Cells. *Adv. Mater.* **26**: 905-909.
6. Gubbala, S., V. Chakrapani, V. Kumar and M.K. Sunkara, (2008). Band-Edge Engineered Hybrid Structures for Dye-Sensitized Solar Cells Based on SnO_2 Nanowires. *Adv*. *Funct*. *Mater*. **18**: 2411-2418.
7. Hong, Y.J., M.Y. Son and Y.C. Kang, (2013). One-Pot Facile Synthesis of Double-Shelled SnO_2 Yolk-Shell-Structured Powders by Continuous Process as Anode Materials for Li-ion Batteries. *Adv. Mater.* **25**: 2279-2283.
8. Ding, J., Z. Li, H. Wang, K. Cui, A. Kohandehghan, X. Tan, D. Karpuzov and D. Mitlin, (2015). Sodiation vs. Lithiation Phase Transformations in a High Rate-high Stability SnO_2 in Carbon Nanocomposite. *J. Mater. Chem. A,* **3**: 7100-7111.
9. Jahel, A., C.M., Ghimbeu, A. Darwiche, L. Vidal, S. Hajjar-Garreau, C. Vix-Guterl and L. Monconduit, (2015). Exceptionally Highly Performing Na-ion Battery Anode Using Crystalline SnO_2 Nanoparticles Confined in Mesoporous Carbon. *J. Mater. Chem. A.* **3**: 11960-11969.
10. Chen, J.S., and X.W. Lou, (2013). SnO_2-Based Nanomaterials: Synthesis and Application in Lithium-Ion Batteries. *Small* **9**: 1877 - 1893.
11. Wang, Z., D. Luan, F.Y.C., Boey and X.W. Lou, (2011). Fast Formation of SnO_2 Nanoboxes with Enhanced Lithium Storage Capability. *J. Am. Chem. Soc.* **133**: 4738-4741.
12. Su, D., C. Wang, H. Ahn and G. Wang, (2013). Octahedral Tin Dioxide Nanocrystals as High Capacity Anode Materials for Na-ion Batteries. *Phys. Chem. Chem. Phys.* **15**: 12543-12550.
13. Han, Y., X. Wu, Y. Ma, L. Gong, F. Qu and H. Fan, (2011). Porous SnO_2 Nanowire Bundles for Photocatalyst and Li ion Battery Applications. *Cryst. Eng. Comm.* **13**: 3506-3510.
14. Wu, H.C., Y.-C. Huang, I.K. Ding, C.-C. Chen, Y.-H. Yang, C.-C. Tsai, C.-D. Chen and Y.-T. Chen, (2011). Photoinduced Electron Transfer in Dye-Sensitized SnO_2 Nanowire Field-Effect Transistors. *Adv. Funct. Mater.* **21**: 474-479.
15. Shin, G., C.H. Yoon, M.Y. Bae, Y.C. Kim, S.K. Hong, J.A. Rogers and J.S. Ha, (2011). Stretchable Field-Effect-Transistor Array of Suspended SnO_2 Nanowires. *Small* **7**: 1181-1185.
16. Oh, H.S., H.N. Nong and P. Strasser, (2015). Preparation of Mesoporous Sb, F, and In-Doped SnO_2 Bulk Powder with High Surface Area for Use as Catalyst Supports in Electrolytic Cells. *Adv. Funct. Mater.* **25**: 1074-1081.
17. Shinde, D.V., D.Y. Lee, S.A. Patil, I. Lim, S.S. Bhande, W. Lee, M.M. Sung, R.S. Mane, N.K. Shrestha and Han, S.-H. (2013). Anodically Fabricated Self-organized Nanoporous Tin Oxide Film as a Supercapacitor Electrode Material. *RSC Adv.* **3**: 9431-9435.
18. Bian, H., Y. Tian, C. Lee, M.F. Yuen, W. Zhang and Y. Yang, (2016). Mesoporous SnO_2 Nanostructures of Ultrahigh Surface Areas by Novel Anodization. *ACS Appl*. *Mater*. *Interfaces* **8**: 28862-28871.
19. Akhila, A.K., P.S., Vinitha and N.K. Renuka, (2018). Photocatalytic Activity of Graphene-Titania Nanocomposite Materials Today: *Proceedings* **5**: 16085-16093.
20. Wang, D., S.C., Pillai, S.-H. Ho, J. Zeng, Y. Li and D.D. Dionysiou, (2018). Plasmonic-based nanomaterials for environmental remediation**.** *Applied Catalysis B: Environmental* **237**: 721-741.
21. Chen, Y., B. Zhai, Y. Liang, Y. Li and Li, J. (2019). Preparation of CdS/ g-C_3N_4/ MOF composite with enhanced visible-light photocatalytic activity for dye degradation. *J. Solid State Chem.* **274**: 32-39.
22. Jiang, L., D. Chen, L. Qin, J. Liang and Y. Huang, (2019). Enhanced photocatalytic activity of hydrogenated $BiVO_4$ with rich surface-oxygen-vacancies for remarkable degradation of tetracycline hydrochloride. *J. Alloys Compd.* **783**: 10-18.
23. Yousaf Khan, M., M. Ahmad, S. Sadaf, S. Iqbal, F. Nawaz and Iqbal, J. (2019). Visible light active indigo dye/graphene/ WO_3 nanocomposites with excellent photocatalytic activity. *J. Mat. Res. Tech,* **8**: 3261-3269.
24. Zhong, N., M. Chen, Y. Luo, Z. Wang, X. Xin and B.E. Rittmann, (2019). A novel photocatalytic optical hollow-fiber with high photocatalytic activity for enhancement of 4-chlorophenol degradation. *Chem. Eng. J.* **355**: 731-739.
25. Wang, T., X. Meng, P. Li, S. Ouyang, K. Chang, G. Liu, Z. Mei and J. Ye, (2014). Photoreduction of CO_2 over the well-crystallized ordered mesoporous TiO_2 with the confined space effect. *Nano Energy* **9**: 50-60.
26. Zhang, Q., P. Liu, C. Miao, Z. Chen, C.M.L. Wu and C. Shek, (2015). Formation of orthorhombic SnO_2 originated from lattice distortion by Mn-doped tetragonal SnO_2. *RSC Adv.* **5**: 39285-39290.